Chinese Chemical Letters 31 (2020) 2651–2656

Contents lists available at ScienceDirect

Chinese Chemical Letters

journal homepage: www.elsevier.com/locate/cclet

Communication

Highly stable and antifouling graphene oxide membranes prepared by bio-inspired modification for water purification

Weiming Zhong, Yuyu Zhang, Ling Zhao, Wanbin Li*

Guangdong Key Laboratory of Environmental Pollution and Health, School of Environment, Jinan University, Guangzhou 511443, China

ARTICLE INFO

Article history:
Received 3 February 2020
Received in revised form 20 February 2020
Accepted 11 March 2020
Available online 12 March 2020

Keywords:
Graphene oxide
Nanofiltration
Polydopamine
Stability
Antifouling

ABSTRACT

Graphene oxide (GO) membranes show great potential in molecular separation for water treatment. However, the inferior stability of GO membranes is a major bottleneck for practical applications. In this study, bio-inspired polydopamine (PDA) deposition is reported for enhancing the stability of GO membranes. Through simple and mild immersion, PDA is self-polymerized on GO membranes. The blocking of PDA chains to membrane defects improves the rejections for various molecules. Because the inherently strong adhesion and crosslinking of PDA greatly strengthen the interactions of substrates to GO layers and the binding force of GO nanosheets, the prepared PDA-GO membranes exhibit impressive long-term stability in cross-flow filtration, and maintain good nanofiltration performance at various feed pressures, tangential velocities, and even after external scratching. Moreover, because the deposited PDA layers obstruct the direct contact between GO and contaminants, the antifouling property of the PDA-GO membranes increases substantially, with recovery ratio about 98%.

The scarcity of fresh water is a serious global issue. One third of the world's population is suffering from the threat of insufficient and insecure drinking water [1] In consideration of the increasing demand for water resource and the aggravation of water pollution, water shortage will get worse in the future [2]. Many technologies are developed to alleviate the water crisis [3]. Membrane separation is one of the most promising technologies because of its advantages of high efficiency, energy saving, no phase change, and easy operation [4]. For membrane technology, membrane materials determine operational efficiency. Polymeric membranes are widely applied for water treatment, due to the merits of excellent processability and low cost. Nevertheless, those membranes are of fouling propensity and chemical sensitivity [5,6]. Besides, the trade-off limitation hinders the further development of polymeric membranes [7]. The exploitation of novel membrane materials is a main research direction in the field of membrane separation.

Graphene oxide (GO), an important derivative of graphene, is applied for miscellaneous applications, owing to its unique 2D structures, adjustable physicochemical characters, and highly mechanical properties. Thanks to the high hydrophilicity, low friction of carbon skeleton in non-oxidized regions, and appropriate transport pathway of 1.0–1.2 nm, GO has commendable implementation in fabrication of nanofiltration membranes with impressive permeability and rejection [8,9]. However, inferior long-term stability is a major bottleneck of GO membranes for water treatment. The combination between GO layers and substrates is mainly depended on electrostatic attractions or other non-covalent bonds. The weak binding force causes the risk of shedding of GO layers from substrates, especially under cross-flow filtration [10–12]. Furthermore, by reason of the hydration and electrostatic repulsion of GO nanosheets, GO membranes commonly swell in aqueous solutions. The attenuation of interaction between nanosheets may eventually result in re-dispersion of GO membranes [13,14]. The instability of GO membranes terribly impedes their applications.

Various modification methods have been exploited to enhance the stability of GO membranes, such as reduction, crosslinking, and physical confinement [10–18]. Reduction improves the stability by decreasing the content of oxygen-containing groups, which may come at the great expense of permeation [17]. Crosslinking refers to the reaction between oxygen-containing groups and introduced reagents, which is usually performed by adding amines in GO suspension for membrane preparation. Zhang *et al.* fabricated the GO composite membranes using ethylene diamine as crosslinking agent. The membranes exhibited high stability in removal of heavy metals [18]. Physical confinement can suppress GO swelling by external force and then effectively improve stability. Recently, we

* Corresponding author.
E-mail address: gandeylin@126.com (W. Li).

https://doi.org/10.1016/j.cclet.2020.03.033

reported that external pressure could endow GO membranes with controllable transport channels and stable desalination performance under cross-flow filtration [19]. But the complicated process of this method is not conducive to separation application. Although a series of progresses have been achieved, the further improvement in stability of GO membranes is still of scientific significance.

As inspired by strong adhesion and self-polymerization of dopamine, improving stability and mechanical properties of various materials by polydopamine (PDA) decoration has been widely investigated [20,21]. PDA layers can be deposited on material surfaces through dopamine self-polymerization under mild conditions [22]. Some studies have reported fabrication of GO membranes by introducing of PDA [23–27]. Xu *et al.* found that PDA could serve as molecular linker between GO and porous Al_2O_3 to obtain high-performance pervaporation membranes [25]. Shen group filtrated dopamine through GO membranes and intercalation-polymerized it in interlayer spaces of GO nanosheets to enhance the stability for desalination [26]. Yang *et al.* grafted PDA on reduced GO membranes to improve the hydrophobicity for forward osmosis [27]. The dopamine was also added in GO suspension to prepare GO-based membranes for adsorption [24]. PDA modification has great potential in preparation of GO nanofiltration membranes with excellent separation stability.

Herein, we employed simple dip-coating to deposit PDA on/in GO membranes for enhancing the stability in nanofiltration. In previous studies, PDA was solely employed as adhesive linker or cross-linker to enhance the stability of GO membranes. Because of the inherently strong adhesion, coating protection, and cross-linking of PDA, after simple dip-coating, the PDA-GO membranes exhibited impressive long-term stability under cross-flow filtration and mechanical stirring. In addition, since PDA prevented GO layers from coming into direct contact with contaminants and reduced the mass transport through the defects of GO layers, the PDA-GO membranes had excellent antifouling property and separation performance.

The GO membrane was fabricated through depositing GO on the mixed cellulose ester microfiltration (MCEM) substrate by vacuum filtration. The morphology of the substrate and GO membranes was characterized by scanning electron microscopy (SEM). As shown in Figs. 1a and b, the substrate had a porous structure with average aperture about 0.2 μm. After GO deposition, the substrate pores were covered, and led to formation of sunk imprints as the small thickness and flexibility of GO layer (Fig. 1c). With the increase of GO concentration, the membranes with greater thickness were more flat, and the imprints became less noticeable (Fig. S1 in Supporting information). From cross-sectional SEM image, the GO membrane showed well-stacked layered structures (Fig. 1d). There was positive correlation between membrane thickness and GO concentration (Fig. S1). The GO membrane prepared with concentration of 100 μg/mL had thickness of 435 nm (Fig. S1f).

For obtaining the PDA-GO membrane, the GO membrane was vertically immersed in dopamine buffer solution with pH of 8.5 and maintained at room temperature for 12 h. After self-polymerization for 12 h, the color of the dopamine solution changed from colorless to brown and a PDA layer was deposited on the GO membrane (Fig. S2 in Supporting information). As presented in Fig. 1e, compared with the GO membrane, the PDA-GO membrane had grainy surface structure, indicating the successful formation of PDA nanoparticles [22]. Since PDA increased the rigidity of flexible GO, the imprints of the PDA-GO membrane were alleviated [20]. The PDA deposition could enable the GO membranes more compact and flat (Figs. S3 and S4 in Supporting information). From the SEM images shown in Figs. 1b–f, the PDA-GO and GO membranes possessed similar asymmetric morphology coupling porous substrates and dense skin layers. The thicknesses of the PDA-GO membranes prepared with concentrations of 100, 50, 25 and 15 μg/mL were approximately 470, 240, 140 and 90 nm, respectively. Compared with the GO membranes, the PDA-GO membranes were slightly thinner. For example, the thickness of the PDA-GO membrane with concentration of 100 μg/mL increased by ~30 nm, suggesting that the deposited PDA was ultrathin, which agreed with the observation in previous studies [22,28].

To further confirm the successful deposition of PDA, the chemical structures of the GO and PDA-GO membranes were characterized by X-ray photoelectron spectroscopy (XPS) and Fourier transform infrared spectroscopy (FTIR). Fig. 2 presents the XPS results of the membranes. Relative to the GO membrane, a new nitrogen peak of the PDA-GO membrane at 399.4 eV appeared,

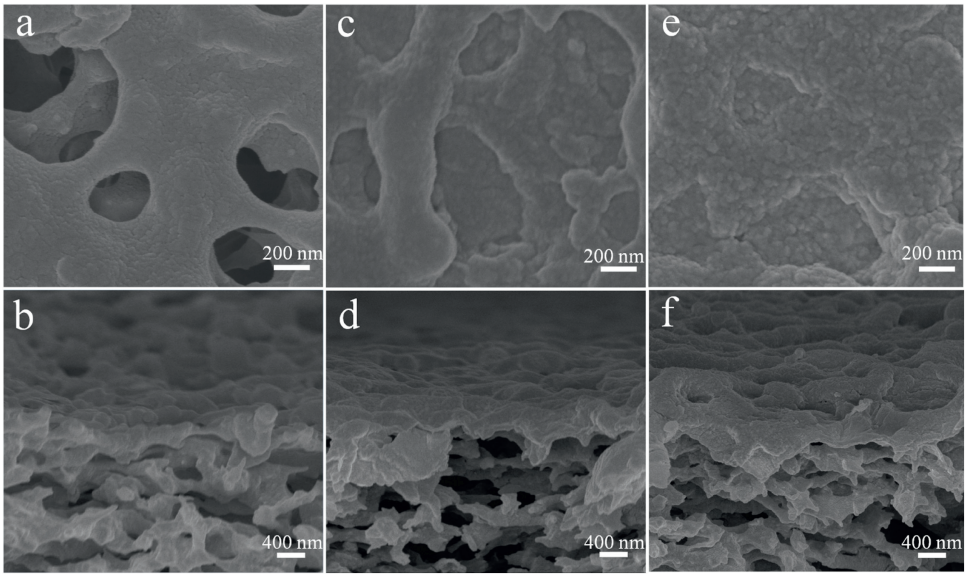

Fig. 1. SEM images of (a, b) the MCEM substrate, (c, d) the GO and (e, f) PDA-GO membranes with GO concentration of 15 μg/mL.

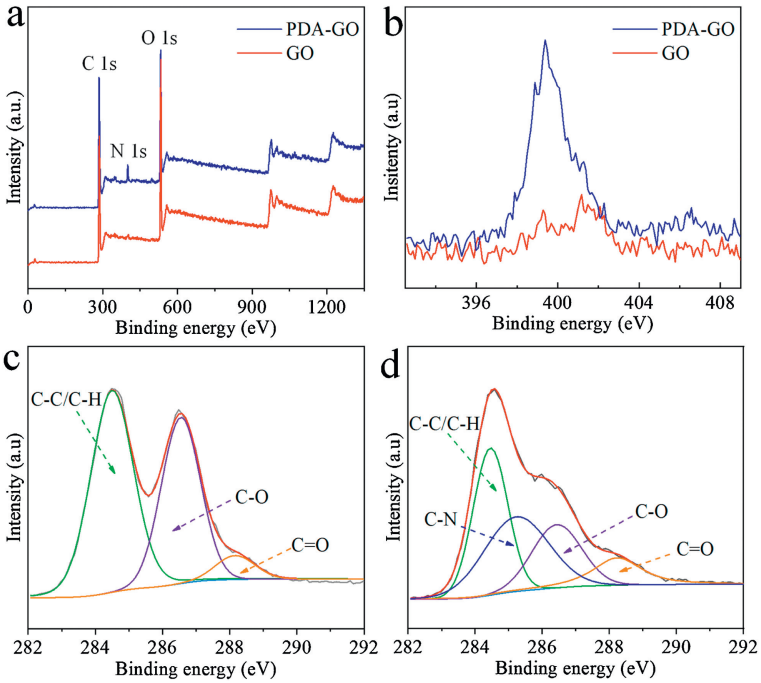

Fig. 2. (a) XPS and (b) high-resolution N 1s XPS spectra of the GO and PDA-GO membranes. High-resolution C 1s XPS spectra of (c) the GO and (d) PDA-GO membranes. The GO and PDA-GO membranes were prepared with GO concentration of 25 μg/mL.

implying the successful PDA deposition. For C 1s XPS spectrum of the GO membrane, three fitting curves with peaks at 284.5, 286.6 and 288.2 eV were assigned to C—C/C—H, C—O and C=O bonds, respectively (Fig. 2c). The emerged C—N peak at 285.3 eV in C 1s XPS spectrum of the PDA-GO membrane confirmed the successful PDA modification as well (Fig. 2d). FTIR characterization displayed that the absorption peak at 3000–3400 cm^{-1} was significantly enhanced due to the introduction of hydroxyl and amino groups from PDA (Fig. S5 in Supporting information). The peak at 1593 cm^{-1} from deformation vibration of N—H in PDA also occurred. The new peak at 1512 cm^{-1} was attributed to the formation of CONH group, indicating the crosslinking between PDA and GO *via* covalent bonds, which may substantially strengthen the stability of the GO membranes. Both XPS and FTIR results demonstrated the successful PDA deposition and membrane crosslinking.

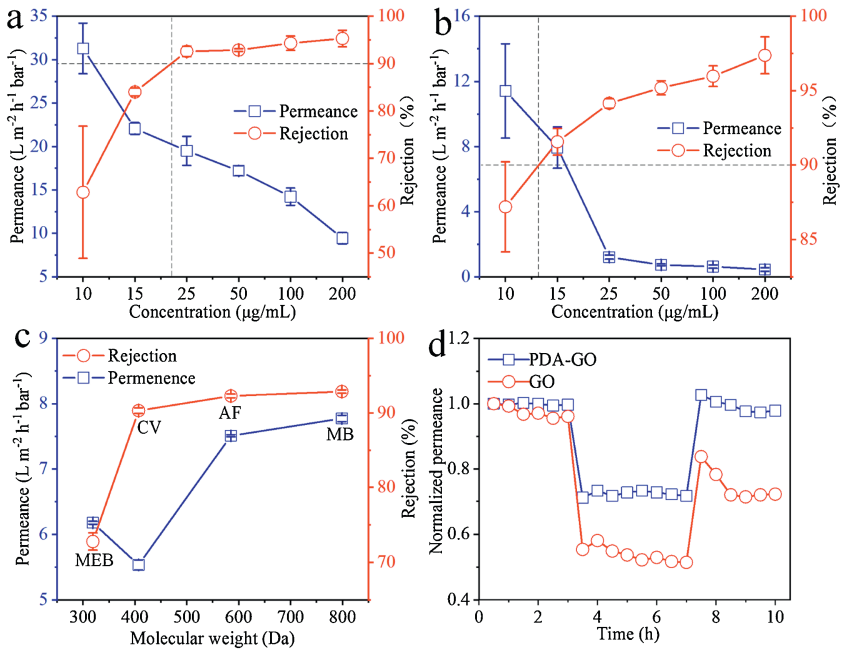

Fig. 3. Separation performance of (a) the GO and (b) PDA-GO membranes prepared with various GO concentrations. (c) Separation performance of the PDA-GO membrane for various dyes. MEB-methylene blue, CV-crystal violet, and AF-acid fuchsin. (d) BSA dynamic fouling experiment of the GO and PDA-GO membranes, 0–3 h, water; 3–7 h, BSA solution; 7–10 h, water.

The permeance and rejection of the as-prepared membranes was investigated by cross-flow filtration, which was widely adopted in practical application. It is well known that the thickness of selective layers immensely affects the separation performance of membranes. As expected, for both GO and PDA-GO membranes, because of larger thickness, the rejection and permeance for methyl blue (MB) solution increased and decreased with the increase of GO concentration, respectively (Figs. 3a and b). Compared with the GO membranes, the PDA-GO membranes with the same GO concentrations had higher rejection but smaller permeance owing to the denser and tighter structures. This was more obvious for the membranes with smaller thicknesses. For example, after PDA deposition, the rejection of the membrane with GO concentration of 10 μg/mL increased from 62.9% (GO) to 87.2% (PDA-GO). This phenomenon was explained by that some defects of the GO membranes were blocked by PDA chains, because more oxygen-containing groups at GO defects promoted preferable PDA self-polymerization [29,30]. Meanwhile, the resulted PDA coats could serve as separation layers, which contributed to the improved rejection as well [31].

The operation conditions have critical impacts on separation performance, especially for GO membranes. The effects of feed pressure and retentate flowrate on separation performance were investigated. Considering the rejection over 90%, the GO membrane with concentration of 25 μg/mL and the PDA-GO membrane with concentration of 15 μg/mL were chosen for comparison in following experiments. The permeance and rejection of two membranes with retentate flowrate of 30 L/h at various pressures were depicted in Figs. S6a and b (Supporting information). Both GO and PDA-GO membranes exhibited smaller permeance at higher feed pressures. The permeance of the GO and PDA-GO membranes decreased by 53.2% (from 15.8 L m^{-2} h^{-1} bar^{-1} at 1.0 bar to 7.4 L m^{-2} h^{-1} bar^{-1} at 7.0 bar) and 37.1% (from 6.2 L m^{-2} h^{-1} bar^{-1} at 1.0 bar to 3.9 L m^{-2} h^{-1} bar^{-1} at 7.0 bar), respectively. The reduction in permeance was interpreted by more compressed transport pathways under higher pressures [32]. The rejection of the GO membrane reduced from 92.6% at 1.0 bar to 82.5% at 5.0 bar, while the PDA-GO membrane had stable rejection about 92% under various feed pressures. The decreased rejection of the GO membrane might be attributed to more serious concentration polarization. As pressure increased, the flux (L m^{-2} h^{-1}), rather than permeance, through the membrane was larger. Thus the concentration polarization became more serious and then led to the degeneration in rejection. However, for the PDA-GO membrane, because PDA enhanced the compactness and diminished the defects, the rejection could be maintained at high level under different pressures. This suggested that the PDA deposition could significantly improve the stability of GO membranes under various feed pressures. Figs. S6c and d (Supporting information) displays the nanofiltration performance of two membranes at 2.0 bar and different retentate flowrates. The larger retentate flowrate means higher tangential velocity and shear force. The greater shear force is more likely to cause the peeling and re-dispersion of GO membranes in solutions. The rejection of both GO and PDA-GO membranes increased slightly as flowrate increased, originated from the alleviated concentration polarization [33]. The permeance exhibited no obvious change. The weak electrostatic interaction and non-covalent bonds between GO layers and substrates may cause the falling of GO layers from substrates under cross-flow conditions [11]. The high hydrophilicity and electronegativity of GO nanosheets bring about the risk of GO re-dispersion in wastewater as well [12,13]. The GO and PDA-GO membranes here exhibited small fluctuations in separation performance under various retentate flowrates. This was ascribed to that the oxygen/amino groups of the MCEM substrate could interact with the GO nanosheets through hydrogen bond and van der Waals force [11], and the imprints of the membranes would also stick the GO layers to prevent them from falling off the substrates. It should be noted, the nanofiltration system was firstly operated for 8 h to reach stable running. For accomplishing the experiment about feed pressure or retentate flowrate, the membrane was further filtrated for another 30 h at least. When the pressure or retentate flowrate was returned to the original one, the permeance of two membranes became smaller due to the increased dye molecules on membrane surfaces after long-term operation. All above results confirmed that the prepared membranes had outstanding long-term stability, and could maintain the performance under various feed pressures and tangential velocities.

To explore the separation mechanism of the membranes, four kinds of different dye solutions with concentration of 100 mg/L were applied to test the separation performance of the prepared membranes. Fig. 3c revealed that the PDA-GO membrane with GO concentration of 15 μg/mL exhibited higher rejection for the molecules with larger molecular weight. This indicated that the PDA-GO membrane was governed by molecular sieving [34]. Because of the similar negative charged property of PDA and GO [35,36], the electronegativity of the PDA-GO membrane might change weakly after modification. The GO membrane exhibited similar tendencies towards various dye molecules (Fig. S7 in Supporting information), implying the same separation mechanism as the PDA-GO membrane. Based on the rejection for different dyes, the molecular weight cutoff (MWCO) of the GO and PDA-GO membranes were estimated as 404 Da and 412 Da, respectively. Theoretically, rejection and permeance have negative correlation. However, the PDA-GO membrane showed simultaneously inferior rejection and permeance for two smaller dyes with positive charge. The possible reason was that the positively charged dyes were easier to adsorb on negatively charged GO membranes [37,38]. Certainly, because same mass concentration led to higher molar concentration for smaller dyes, more serious concentration polarization also resulted in smaller permeance [33,39]. Therefore, it was deduced that the rejection was mainly governed by molecular sieving, while the permeance was influenced by Dounan effect and sieving synergistically.

Membrane fouling can tremendously degrade the service life and separation efficiency of membranes [5]. We evaluated the antifouling property of the prepared membranes through employing the most commonly used bovine serum albumin (BSA) as a model pollutant. As shown in Fig. 3d, after replacing feed water by BSA solution, the GO membrane displayed a drastic reduction of 46.0% in permeance. Comparatively, the decrement of 27.6% in permeance of the PDA-GO membrane was much lower. After simple shaking in water, the permeance of the PDA-GO membrane was recovered to 97.9% of the original one, but the recovery ratio of the GO membrane was only 74.7%. It should be noted that, because the filtration was operated for 8 h to achieve stability, while the permeance after cleaning was tested without stabilization, the first normalized permeance after shaking was slightly greater than 1.0. Accordingly, the irreversible fouling rates of the PDA-GO and GO membranes were 2.1% and 25.3%, respectively. In other words, the fouling of the PDA-GO membrane was reversible, but a large part of permeance reduction of the GO membrane was irreversible. These results indicated that the antifouling property of the membrane was improved substantially by PDA deposition. It is well-known that higher hydrophilicity and lower roughness usually imply better antifouling property. The hydrophilicity of the membranes was measured by water contact angle. After modification, all PDA membranes with various GO concentrations had poorer hydrophilicity than the GO membranes, which could be identified by the larger contact angle (Fig. S8 in Supporting information). The main

reason for affecting antifouling feature should not be membrane hydrophilicity. As demonstrated in previous studies, there was strong interaction between BSA and GO materials [40–42]. The interaction might greatly increase the enrichment of BSA on GO surface and then reduced water permeance. The strong interaction would result in poor permeance recovery simultaneously. After self-polymerization, PDA could obstruct the direct contact between GO and BSA and thus improve the antifouling property of the PDA-GO membrane. Also, the alleviated imprints might play certain effect for the better antifouling property.

The outstanding stability of membranes is a prerequisite for separation applications. The instability of GO membranes not only negatively affects the separation performance, but also the dispersion of GO sheets in water will cause potential harm to environments [43]. Therefore, the robust stability of GO membranes is crucial. The stability of the GO and PDA-GO membranes was further investigated by the variation in nanifiltration performance before and after external scratching. In the actual cleaning and application process, separation membranes are inevitable to be subjected to external scratching [25,44]. During membrane preparation, we found that the GO membranes were hard to maintain intact even with soft finger touch. As observed from Fig. 4, the wetted GO and PDA-GO membranes showed brown color in water. After subjecting to stirring by rotor at 200 rpm, the area of the GO membrane that contacted with rotor was lighter, suggesting the falling of GO sheets. With the progress of processing, the peeled area became wider. However, for the PDA-GO membrane, the color showed no obvious change after processing, revealing that PDA deposition could effectively enhance the mechanical stability. The separation performance of two membranes after processing for 15 min was measured. The rejection of the GO membrane degraded by 28.8% (from 92.6%–63.8%), and the permeance increased by 79.1%. Fortunately, both rejection and permeance of the PDA-GO membrane displayed no significant variations. The rejection was still stable around 90%. Even extending the processing time to 30 min, the PDA-GO membrane still showed intact morphology and good separation performance (Fig. S9 in Supporting information). The stability of two membranes could also be differentiated from the photographs before and after nanofiltration (Fig. S10 in Supporting information). The GO membranes showed serious GO shedding after pressing by o-ring. In contrast, the PDA-GO layers were intact, despite the existence of o-ring indentations. For GO membranes, the interaction between GO sheets was relatively weak due to the hydration and electrostatic repulsion in aqueous solutions. The GO layers would detach from substrates after external scratching. After immersion in the dopamine buffer solution, a strong adhesion layer could be formed not only on the surface of membranes but also at the interface between substrates and GO layers to enhance the anchoring strength. Moreover, the crosslinking between GO and PDA reinforced the interaction between GO nanosheets. Therefore, the PDA-GO membranes exhibited much better mechanical stability. In addition to mechanical stability, the PDA-GO membrane displayed excellent stability under various pH values as well (Fig. S11 in Supporting information).

In summary, we demonstrated that the PDA deposition could significantly improve the stability of GO membranes. Due to the strong adhesion as “bioglue” and the crosslinking of PDA to GO, the interactions of GO nanosheets and between GO layers and substrates were enhanced significantly. The PDA-GO membranes showed impressive stability under high pressure, large tangential velocity, and even after external scratching. The performance could be maintained after long-term filtration under variable operation conditions. Meanwhile, the formed PDA chains could refine the defects of the GO membranes and increase the rejection for various small molecules. Furthermore, the PDA-GO membranes had excellent antifouling property, with recovery ratio about 98% after BSA fouling. Although the researches on graphene-based membranes are in its infancy and there various shortcomings should be solved, we humbly believe that this work provides an alternative

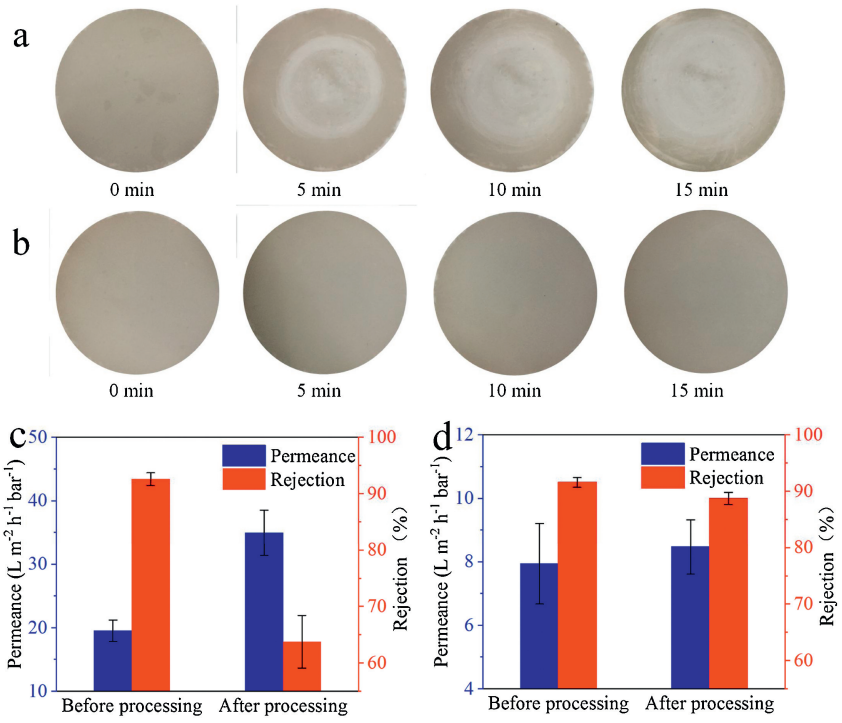

Fig. 4. (a,b) Photographs and (c,d) separation performance of (a,c) the GO and (b,d) PDA-GO membranes after external scratching by mechanical stirring.

route to overcome the poor antifouling and stability of GO membranes.

Declaration of competing interest

The authors declare that they have no known competing financial interests or personal relationships that could have appeared to influence the work reported in this paper.

Acknowledgments

This work was financially supported by the National Natural Science Foundation of China (No. 51708252) and the Fundamental Research Funds for the Central Universities (No. 21617322).

Appendix A. Supplementary data

Supplementary material related to this article can be found, in the online version, at doi:https://doi.org/10.1016/j.cclet.2020.03.033.

References

[1] R.F. Service, Science 313 (2006) 1088–1090.
[2] C.J. Vorosmarty, P.B. McIntyre, M.O. Gessner, et al., Nature 467 (2010) 555–561.
[3] M.A. Shannon, P.W. Bohn, M. Elimelech, et al., Nature 452 (2008) 301–310.
[4] J. Li, S. Li, X. Wang, et al., Chin. Chem. Lett. 30 (2019) 239–242.
[5] M. Nystrom, L. Kaipia, S. Luque, J. Membr. Sci. 98 (1995) 249–262.
[6] K.L. Cho, A.J. Hill, F. Caruso, S.E. Kentish, Adv. Mater. 27 (2015) 2791–2796.
[7] G.M. Geise, H.B. Park, A.C. Sagle, B.D. Freeman, J.E. McGrath, J. Membr. Sci. 369 (2011) 130–138.
[8] J. Abraham, K.S. Vasu, C.D. Williams, et al., Nat. Nanotech. 12 (2017) 546–550.
[9] L. Chen, G. Shi, J. Shen, et al., Nature 550 (2017) 380–383.
[10] K. Goh, W. Jiang, H.E. Karahan, et al., Adv. Funct. Mater. 25 (2015) 7348–7359.
[11] A. Morelos-Gomez, R. Cruz-Silva, H. Muramatsu, et al., Nat. Nanotechnol. 12 (2017) 1083–1088.
[12] K.H. Thebo, X. Qian, Q. Zhang, et al., Nat. Commun. 9 (2018) 1486.
[13] C.N. Yeh, K. Raidongia, J. Shao, Q.H. Yang, J. Huang, Nat. Chem. 7 (2015) 166–170.
[14] S. Zheng, Q. Tu, J.J. Urban, S. Li, B. Mi, ACS Nano 11 (2017) 6440–6450.
[15] Y. Wei, Y. Zhang, X. Gao, et al., Carbon 139 (2018) 964–981.
[16] W. Wu, J. Su, M. Jia, et al., J. Mater. Chem. A 7 (2019) 13007–13011.
[17] H. Liu, H. Wang, X. Zhang, Adv. Mater. 27 (2015) 249–254.
[18] Y. Zhang, S. Zhang, T.S. Chung, Environ. Sci. Technol. 49 (2015) 10235–10242.
[19] W. Li, W. Wu, Z. Li, ACS Nano 12 (2018) 9309–9317.
[20] Y. Liu, K. Ai, L. Lu, Chem. Rev. 114 (2014) 5057–5115.
[21] Y. Zhang, M. Qi, R. Fu, Chin. Chem. Lett. 27 (2016) 88–90.
[22] H. Lee, S.M. Dellatore, W.M. Miller, P.B. Messersmith, Science 318 (2007) 426–430.
[23] Y. Qian, C. Zhou, A. Huang, Carbon 136 (2018) 28–37.
[24] J. Wang, T. Huang, L. Zhang, Q.J. Yu, L. Hou, Environ. Technol. 39 (2018) 3055–3065.
[25] K. Xu, B. Feng, C. Zhou, A. Huang, Chem. Eng. Sci. 146 (2016) 159–165.
[26] Y. Xu, M. Wu, S. Yu, et al., J. Membr. Sci. 586 (2019) 15–22.
[27] E. Yang, C.M. Kim, J. Song, et al., Carbon 117 (2017) 293–300.
[28] W. Wu, Z. Li, Y. Chen, W. Li, Environ. Sci. Technol. 53 (2019) 3764–3772.
[29] X.Q. Cheng, C. Zhang, Z.X. Wang, L. Shao, J. Membr. Sci. 499 (2016) 326–334.
[30] H. Lee, J. Rho, P.B. Messersmith, Adv. Mater. 21 (2009) 431–434.
[31] C. Zhang, Y. Lv, W.Z. Qiu, A. He, Z.K. Xu, ACS Appl. Mater. Interfaces 9 (2017) 14437–14444.
[32] H. Huang, Y. Mao, Y. Ying, et al., Chem. Commun. 49 (2013) 5963–5965.
[33] X.Q. Cheng, Z.X. Wang, Y. Zhang, et al., J. Membr. Sci. 554 (2018) 385–394.
[34] Y. Han, Z. Xu, C. Gao, Adv. Funct. Mater. 23 (2013) 3693–3700.
[35] Y. Li, S. Shi, H. Cao, et al., J. Membr. Sci. 566 (2018) 44–53.
[36] H.M. Hegab, A. ElMekawy, T.G. Barclay, et al., Desalination 385 (2016) 126–137.
[37] W. Choi, J. Choi, J. Bang, J.H. Lee, ACS Appl. Mater. Interfaces 5 (2013) 12510–12519.
[38] H. Ruan, Z. Zheng, J. Pan, et al., J. Membr. Sci. 550 (2018) 427–435.
[39] Y. Zhang, S. Ni, X. Wang, et al., Chem. Eng. J. 372 (2019) 82–91.
[40] T. Kavitha, I.K. Kang, S.Y. Park, Langmuir 30 (2014) 402–409.
[41] Q. Liu, J. Shi, M. Cheng, et al., Chem. Commun. 48 (2012) 1874–1876.
[42] J. Kuchlyan, N. Kundu, D. Banik, A. Roy, N. Sarkar, Langmuir 31 (2015) 13793–13801.
[43] J. Zhao, Z. Wang, J.C. White, B. Xing, Environ. Sci. Technol. 48 (2014) 9995–10009.
[44] B. Van der Bruggen, M. Manttari, M. Nystrom, Sep. Purif. Technol. 63 (2008) 251–263.